Research in Astron. Astrophys. **2013** Vol. **13** No. **10**, 1219–1224
http://www.raa-journal.org *http://www.iop.org/journals/raa*

Research in Astronomy and Astrophysics

The properties of solar active regions responsible for ground level enhancements during solar cycles 22 and 23 *

Gui-Ming Le[1,2], Peng Li[3], Hui-Gen Yang[2], Yu-Lin Chen[3], Xing-Xing Yang[3] and Zhi-Qiang Yin[4]

[1] National Center for Space Weather, China Meteorological Administration, Beijing 100081, China; *legm@cma.gov.cn*
[2] SOA Key Laboratory for Polar Science, Polar Research Institute of China, Shanghai 200136, China
[3] Nanjing University of Information Science & Technology, Nanjing 210044, China
[4] National Astronomical Observatories, Chinese Academy of Sciences, Beijing 100012, China

Received 2013 March 11; accepted 2013 May 9

Abstract This is a study designed to analyze the relationship between ground level enhancements (GLEs) and their associated solar active regions during solar cycles 22 and 23. Results show that 90.3% of the GLE events that are investigated are accompanied by X-class flares, and that 77.4% of the GLE events originate from super active regions. It is found that the intensity of a GLE event is strongly associated with the specific position of an active region where the GLE event occurs. As a consequence, the GLE events having a peak increase rate exceeding 50% occur in a longitudinal range from W20° to W100°. Moreover, the largest GLE events occur in a heliographic longitude at roughly W60°. Additionally, an analysis is made to understand the distributional pattern of the Carrington longitude of the active regions that have generated the GLE events.

Key words: Sun: particle emission — Sun: flares — Sun: sunspots

1 INTRODUCTION

Solar energetic particles (SEPs), or solar cosmic rays (SCRs) are particles accelerated at/near the Sun to energies greater than 10 keV (Miroshnichenko 2001). Ground level enhancements (GLEs) are the increases of SCR intensity measured by ground-based neutron monitors. Shea & Smart (2012) pointed out that protons with energies greater than approximately 450 MeV can generate a nuclear cascade that can penetrate to the surface of the Earth in the polar regions. A particle with energy of 450 MeV would have a rigidity of 1.03 GV according to the relationship between rigidity and the energy of a particle (Le et al. 2006). The protons from GLE events have very high energy and can pose serious threats to the functionality of satellites and to the safety of astronauts working in space (Shea & Smart 2012). In fact, GLE events probably only account for 15% of the total number of

* Supported by the National Natural Science Foundation of China.

solar proton events in each solar cycle (Shea & Smart 2012). This is similar to the ratio of great geomagnetic storms to the total number of major geomagnetic storms (Le et al. 2013). Both GLE events and great geomagnetic storms (Le et al. 2012) are important phenomena in space weather, and we should pay great attention to them.

A GLE event would always be accompanied by the eruption of a strong flare and a fast halo or partial halo coronal mass ejection (CME) in the same active region. Scientists have not yet reached consensus on which one, flare or CME, is the dominant player in a GLE event (Cane et al. 2006; Li et al. 2007a,b, 2009, 2012; Andriopoulou et al. 2011; Firoz et al. 2012; Gopalswamy et al. 2012; Kahler et al. 2012; Miroshnichenko et al. 2005a,b; Moraal & McCracken 2012; Nitta et al. 2012). More observations are needed, especially for cases closer to the Sun, to understand the acceleration mechanism of relativistic energetic particles (Le et al. 2008).

The concept of a super active region (SAR) was first proposed by Bai (1987). The major flare number, the flare index, the largest area of the active region (AR), the maximum 10.7 cm radio flux, the short-term decrease in total solar irradiance (ΔTSI), the peak flux of a solar proton event and the geomagnetic Ap index associated with the solar proton event produced by the AR can be used to judge whether or not the AR is an SAR. The different criteria for describing an SAR have been adopted by different authors and are described in detail by Chen et al. (2011). If an AR satisfies three of the four criteria, including the largest area of the $\mathrm{AR} > 1000$ μh, flare index > 10, 10.7 cm peak flux > 1000 s.f.u. and $\Delta\mathrm{TSI} < -0.1\%$, then the AR is defined as an SAR by Chen et al. (2011). 45 ARs selected by Chen et al. (2011) as SARs during solar cycles 21–23 were listed in appendix A of their paper. It is worth noting that we directly use data from the 45 SARs selected by Chen et al. (2011) as our criteria to judge whether or not an AR is an SAR.

Firoz et al. (2011) pointed out that most GLE events took place during an X class flare. Taking into account the fact that about 50% of X-class flares originate from SARs, one would therefore assume that some GLE events are inevitably the makings of SARs, though SARs would be defined somewhat differently (Roy 1977; Bai 1987, 1988; Wu & Zhang 1995; Li & Wang 1997; Tian et al. 2002; Romano & Zuccarello 2007; Wang et al. 2011; Chen et al. 2011). Now the question is how many GLE events originate from SARs? This study will analyze some features of SARs that have generated GLE events during solar cycles 22 and 23. Section 2 presents the data analysis. Section 3 is dedicated to conclusions and discussion.

2 DATA ANALYSIS

The GLE events analyzed in this study are the 40^{th}–70^{th} GLE events identified by the Oulu Cosmic Ray Station during solar cycles 22 and 23. In Table 1, each GLE event is numbered in column (1), with peak increase rate (PIR) in column (2), date in column (3), (X-ray/Hα) for the solar flare in column (4), basic information on where the flare occurred, in terms of heliographic position, in column (5), the NOAA number of the AR in column (6), the largest area of the AR in column (7), the sky speed and width in columns (8) and (9) respectively, the Carrington longitude in column (10), and whether or not there was an SAR for the given event in column (11).

Because the CME data of solar cycle 22 are not available, only the CME information that was collected in solar cycle 23 is presented in Table 1. The CME information describing solar cycle 23 in Table 1 is directly copied from the paper of Gopalswamy et al. (2012). According to the CME information in Table 1, one can find a relationship between SARs and CME speed: SARs produce CMEs that have a higher speed than those produced by normal ARs.

One can see in Table 1 that solar cycles 22 and 23 produced 31 GLE events. Of them, 24 events originated from SARs, or 77.4% of the total. Meanwhile, seven GLE events came from non-SARs, or 22.6%. In this context, the majority of GLE events that occurred in solar cycles 22 and 23 originated from SARs. It can be seen from Figure 1 that all the GLE events with peak increase rates equal to or higher than 10% were caused by SARs.

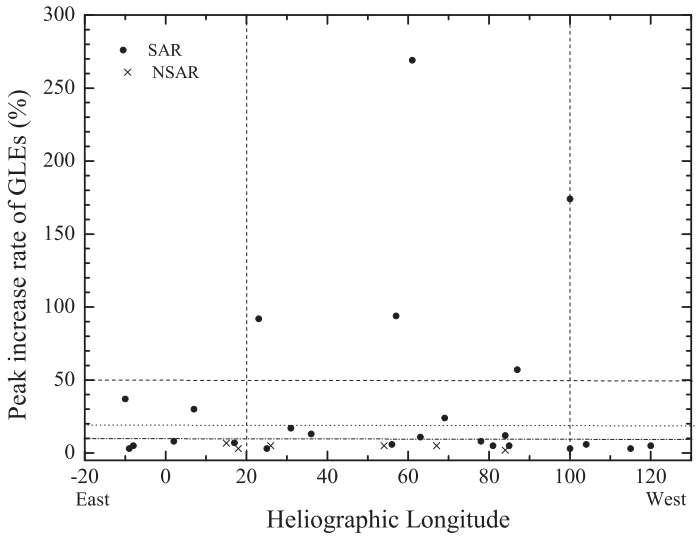

Fig. 1 GLE events' peak increase rate by heliographic longitude.

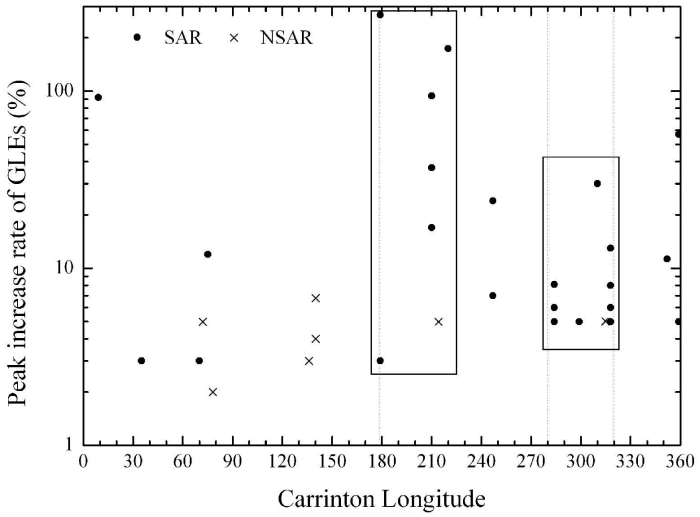

Fig. 2 Distribution of the Carrington longitude for the ARs that have generated GLE events.

Table 1 shows the distribution of heliographic longitude for the ARs that have generated GLE events with different peak increase rates, with more details shown in Figure 1. From Figure 1, one can see that the ARs having peak increase rates exceeding 20% are positioned in a range of heliographic longitude from E10° to W100°, but the ones claiming to have peak increase rates surpassing 50% are distributed in the longitude range from W20° to W100°, with the GLE event showing the largest peak increase rate being located at roughly W60°, which suggests there is a significant relationship between the intensity of the GLE events and the location of the source regions.

Table 1 GLEs in Solar Cycles 22 and 23 and the Associated ARs and Flares.

GLE No.	PIR (%)	Date yyyymmdd	Solar flare X-ray/Hα	Active Region Location	NOAA No.	Smax[a] (μh)	CME Sky Speed (km s^{-1})	CME Angular width (°)	CL[b]	SAR
(1)	(2)	(3)	(4)	(5)	(6)	(7)	(8)	(9)	(10)	(11)
40	2	1989.07.25	X2.6/2N	N25W84	5603	180	–	–	78	No
41	12	1989.08.16	X20/2N	S18W84	5629	1250	–	–	75	Yes
42	174	1989.09.26	X9.8/1B	S26W100	5698	1180	–	–	220	Yes
43	37	1989.10.19	X13/4B	S27E10	5747	1100	–	–	210	Yes
44	17	1989.10.22	X2.9/2B	S27W31	5747	1100	–	–	210	Yes
45	94	1989.10.24	X5.7/3B	S30W57	5747	1100	–	–	210	Yes
46	5	1989.11.15	X3.2/3B	N11W26	5786	510	–	–	72	No
47	13	1990.05.21	X5.5/2B	N25W36	6063	790	–	–	318	Yes
48	8	1990.05.24	X9.3/1B	N33W78	6063	790	–	–	318	Yes
49	6	1990.05.26	X1.4/?	N33W78	6063	790	–	–	318	Yes
50	5	1990.05.28	C9.7/?	N33W120	6063	790	–	–	318	Yes
51	7	1991.06.11	X12/3B	N31W17	6659	2300	–	–	247	Yes
52	24	1991.06.15	X12/3B	N33W69	6659	2300	–	–	247	Yes
53	5	1992.06.25	X3.9/2B	N09W67	7205	1230	–	–	315	No
54	3	1992.11.02	X9.0/0	S25W100	7321	1580	–	–	70	Yes
55	11.3	1997.11.06	X9.4/2B	S18W63	8100	1000	1556	360	352	Yes
56	6.8	1998.05.02	X1.1/3B	S15W15	8210	480	935	360	140	No
57	4	1998.05.06	X2.7/1N	S11W65	8210	480	1099	190	140	No
58	3	1989.08.24	X1.0/3B	N35E09	8307	570	DG*	DG	35	Yes
59	30	2000.07.14	X5.7/3B	N22W07	9077	1010	1674	360	310	Yes
60	57	2001.04.15	X14/2B	S20W85	9415	880	1199	167	359	Yes
61	5	2001.04.18	C2.2/?	S20W115	9415	880	2465	360	359	Yes
62	3	2001.11.04	X1.0/3B	N06W18	9684	510	1810	360	136	No
63	5	2001.12.26	M7.1/1B	N08W54	9742	1070	1446	>212	214	No
64	5	2002.08.24	X3.1/1F	S02W81	10069	1990	1913	360	299	Yes
65	5	2003.10.28	X17/4B	S16E08	10486	2370	2459	360	284	Yes
66	8.1	2003.10.29	X10/2B	S15W02	10486	2370	2029	360	284	Yes
67	6	2003.11.02	X8.3/2B	S14W56	10486	2370	2598	360	284	Yes
68	3	2005.01.17	X3.8/3B	N15W25	10720	1630	2547	360	179	Yes
69	269	2005.01.20	X7.1/2B	N14W61	10720	1630	3242	360	179	Yes
70	92	2006.12.13	X3.4/4B	S06W23	10930	680	1774	360	9	Yes

[a]: Smax, the largest area of the AR; [b]: CL, Carrington longitude; $*$: DG, data gap.

Table 1 also shows the distribution of Carrington longitude for the ARs that generated GLEs, with more details given in Figure 2. We use NSAR to indicate a non-SAR in this paper, as shown in Figure 2. One can see that the ARs that have generated GLE events are mainly distributed in several Carrington longitude regions. Among them, two regions of longitude deserve special attention. One is the black rectangular region ranging from 179° to 220°, having the largest peak increase rate. The other is the black rectangular region covering an area from 280° to 320°, featuring the most intensive ARs that can generate GLEs. One can also spot some individual GLE events in some other regions. Each region may have 2–4 GLE events.

3 CONCLUSIONS AND DISCUSSION

The following conclusions have been reached through the above analysis.

(1) In solar cycles 22 and 23, 77.4% of the GLE events originate from the SARs, with 22.6% from NSARs. All the GLEs with peak increase rates exceeding 10% are produced by SARs.

(2) The ARs that generated GLEs with peak increase rates exceeding 20% were positioned in a heliographic longitude range from E10° to W100°, but the ones that generated GLEs with peak increase rates surpassing the threshold of 50% range from W20° to W100°. The ARs producing the GLE events with highest peak increase rates were roughly located at W60°.
(3) The ARs that are distributed in the Carrington longitude from 179° to 220° generate the GLE events having the largest peak increase rate, but the ones in the range from 280° to 320° would see the most dense or intensive ARs that can generate GLEs.

Table 1 shows that of the 31 GLE events that occurred during cycles 22 and 23, 28 events are associated with the presence of X-class flares, suggesting that 90.3% of the GLE events would be accompanied by X-class flares. Nearly 50% of the flares in X-class or above originated from the SARs. Evidently, one can conclude that SARs are closely associated with the incidences of GLE events during cycles 22 and 23, which is consistent with the fact that 77.4% of the GLE events that occurred in solar cycles 22 and 23 originated from SARs.

This study confirms the significant link between the intensity of a GLE event and the heliographic longitude of an AR where the GLE event occurs. The AR located at about W60° that generated the strongest GLE event, in particular, implies there is an extremely important role played by flares in triggering some GLE events. Considering the fact that it would take some 27 days for the Sun to complete a rotation, the footpoint of the Parker field line connected to the Earth will be located at W56°, which is basically consistent with the view of Nitta et al. (2012), namely "the Western Hemisphere, centered around the longitude of W60°, is usually thought of as being well-connected." However, the location of the footpoint of the Parker field line on the Sun, which connects the Sun and the Earth, calculated with the real solar wind speed at the time when the GLE events took place, sometimes shows a relatively large gap from the position of the AR. For example, during the GLE event that took place on 2005 January 20, the gap reached 34° (Nitta et al. 2012). A GLE event is always accompanied by solar flares and a fast halo or partial halo CME. The occurrence of a fast halo or partial halo CME would lead to the global disturbances, which in turn would result in global magnetic reconstruction (Chen 2011; Schrijver & Title 2011). When the Sun is quiet, the situation of a Parker spiral field line close to the Sun will be somewhat different from one when a strong eruption is taking place on the Sun.

The CME-driven shock can also accelerate particles to GeV energies. Meanwhile, particles move along a Parker spiral field line in interplanetary space, which may explain the physical cause behind the phenomenon shown in Figure 1, namely that ground neutron monitors can observe particles with relativistic energies that originate from the source in the eastern AR; however, the events having peak increase rates exceeding 50% are produced by the eruption of the AR, which has a longitude range from W20° to W100°.

Acknowledgements The GLE data used in this paper are obtained from the Oulu cosmic ray station (*http://wdc.kugi.kyoto-u.ac.jp/dstdir/*). This work is supported by the National Basic Research Program of China (973 Program, Grant Nos. 2012CB957801 and 2011CB811406), the National Natural Science Foundation of China (Grant Nos. 41074132, 41274193, 40931056 and 41031064), the National Standard Research Program (Grant No. 10-123) and the program SOA Key Laboratory for Polar Science, Polar Research Institute of China (Grant No. KP201206).

References

Andriopoulou, M., Mavromichalaki, H., Plainaki, C., Belov, A., & Eroshenko, E. 2011, Sol. Phys., 269, 155
Bai, T. 1987, ApJ, 314, 795
Bai, T. 1988, ApJ, 328, 860
Belov, A. V., Eroshenko, E. A., Kryakunova, O. N., Kurt, V. G., & Yanke, V. G. 2010, Geomagnetism and Aeronomy, 50, 21

Cane, H. V., Mewaldt, R. A., Cohen, C. M. S., & von Rosenvinge, T. T. 2006, Journal of Geophysical Research (Space Physics), 111, A06S90
Chen, A. Q., Wang, J. X., Li, J. W., Feynman, J., & Zhang, J. 2011, A&A, 534, A47
Chen P. F., Living Rev., 2011, Solar Phys, 159, 19
Firoz, K. A., Moon, Y.-J., Cho, K.-S., et al. 2011, Journal of Geophysical Research (Space Physics), 116, A04101
Firoz, K. A., Gan, W. Q., Moon, Y.-J., & LI, C. 2012, ApJ, 758, 119
Gopalswamy, N., Xie, H., Yashiro, S., et al. 2012, Space Sci. Rev., 171, 23
Kahler, S. W., Cliver, E. W., Tylka, A. J., & Dietrich, W. F. 2012, Space Sci. Rev., 171, 121
Le, G.-M., Tang, Y.-H., & Han, Y.-B. 2006, ChJAA (Chin. J. Astron. Astrophys.), 6, 751
Le, G., Tang, Y., & Han, Y. 2008, Chinese Science Bulletin, 53, 161
Le, G., Cai, Z., Wang, H., & Zhu, Y. 2012, Ap&SS, 339, 151
Le, G. M., Cai, Z.-Y., Wang, H.-N., & Li, P. 2013, RAA (Research in Astronomy and Astrophysics), 13, 739
Li, W., & Wang, H. 1997, Publications of the Yunnan Observatory, 1, 10
Li, C., Tang, Y. H., Dai, Y., Fang, C., & Vial, J.-C. 2007a, A&A, 472, 283
Li, C., Tang, Y. H., Dai, Y., Zong, W. G., & Fang, C. 2007b, A&A, 461, 1115
Li, C., Dai, Y., Vial, J.-C., et al. 2009, A&A, 503, 1013
Li, G., Moore, R., Mewaldt, R. A., Zhao, L., & Labrador, A. W. 2012, Space Sci. Rev., 171, 141
Miroshnichenko, L. I., ed. 2001, Solar Cosmic Rays, Astrophysics and Space Science Library, 260 (Kluwer Academic Publishers)
Miroshnichenko, L. I., Klein, K.-L., Trottet, G., et al. 2005a, Journal of Geophysical Research (Space Physics), 110, A09S08
Miroshnichenko, L. I., Klein, K.-L., Trottet, G., et al. 2005b, Advances in Space Research, 35, 1864
Moraal, H., & McCracken, K. G. 2012, Space Sci. Rev., 171, 85
Nitta, N. V., Liu, Y., DeRosa, M. L., & Nightingale, R. W. 2012, Space Sci. Rev., 171, 61
Romano, P., & Zuccarello, F. 2007, A&A, 474, 633
Roy, J.-R. 1977, Sol. Phys., 52, 53
Schrijver, C. J., & Title, A. M. 2011, Journal of Geophysical Research (Space Physics), 116, A04108
Shea, M. A., & Smart, D. F. 2012, Space Sci. Rev., 171, 161
Tian, L., Liu, Y., & Wang, J. 2002, Sol. Phys., 209, 361
Wang, J. X., Chen, A. Q., Feynman, J., et al. 2011, in Proc. IAU Symp. 273
Wu, M., & Zhang, Q. 1995, Publications of the Yunnan Observatory, 1, 1